*Meteoritics & Planetary Science* 37, 1797–1813 (2002)
Available online at http://www.uark.edu/meteor

# Northwest Africa 482: A crystalline impact-melt breccia from the lunar highlands

INGRID J. DAUBAR[1], DAVID A. KRING[1]*, TIMOTHY D. SWINDLE[1] AND A. J. TIMOTHY JULL[2]

[1]Lunar and Planetary Laboratory, University of Arizona, Tucson, Arizona, 85721, USA
[2]NSF AMS Facility, University of Arizona, Tucson, Arizona, 85721, USA
*Correspondence author's e-mail address: kring@LPL.arizona.edu

*(Received 2002 April 11; accepted in revised form 2002 August 21)*

**Abstract**–Northwest Africa 482 (NWA 482) is a crystalline impact-melt breccia from the Moon with highlands affinities. The recrystallized matrix and the clast population are both highly anorthositic. Clasts are all related to the ferroan anorthosite suite, and include isolated plagioclase crystals and lithic anorthosites, troctolites, and spinel troctolites. Potassium-, rare-earth-element-, and phosphorus-bearing (KREEP) and mare lithologies are both absent, constraining the source area of this meteorite to a highland terrain with little to no KREEP component, most likely on the far side of the Moon. Glass is present in shock veins cutting through the sample and in several large melt pockets, indicating a second impact event.

There are two separate events recorded in the $^{40}Ar$-$^{39}Ar$ system: one at ~3750 Ma, which completely reset the K-Ar system, and one at $\lesssim$2400 Ma, which caused only partial degassing. These events could represent, respectively, crystallization of the impact-melt breccia and later formation of the glass, or the formation of the glass and a later thermal event.

The terrestrial age of the meteorite is 8.6 ± 1.3 ka. This age corresponds well with the modest amount of weathering in the rock, in the form of secondary phyllosilicates and carbonates. Based on terrestrial age and location, lithology, and chemistry, NWA 482 is unique among known lunar meteorites.

## INTRODUCTION

Northwest Africa 482 (NWA 482) is the second largest lunar meteorite and the fifth found in the Sahara. The complete stone had a mass of 1.015 kg before cutting; it alone represents 13% of the total mass of known lunar meteorites. Michael Farmer purchased the meteorite in January 2001 in Alnif, Morocco (Grossman and Zipfel, 2001). As with many other Northwest Africa meteorites, its exact fall location is unknown, although it is assumed to have been found somewhere nearby in the Sahara.

Preliminary examination of the meteorite by our group and another at UCLA led to a classification as a crystalline impact-melt breccia (Grossman and Zipfel, 2001; Warren and Kallemeyn, 2001).

## METHODS

We sliced the meteorite to produce a 4.5 mm thick slab (Fig. 1). This slice was cut into an approximate rectangle (12.31 g) that included the two melt pockets visible in Fig. 1. Two polished thin sections were made out of this split, each about 23 × 40 mm. One was carbon coated and used for optical and electron microscopy; the other remains untouched. From the slab, we kept 2.33 g for other analyses, and the remainder was returned to the owner. Two splits were taken for $^{40}Ar$-$^{39}Ar$ analysis: 6.40 mg from the bulk rock, as free as possible from shock melt, and a 2.88 mg sample of shock glass from one of the melt veins in the thin-section block. Another split of 318.5 mg from the bulk sample was prepared for $^{14}C$ analysis. These splits were chosen to avoid the edge of the slice, in order to minimize possible contamination from the fusion crust, external contamination, and any thermal effects concentrated near the outside of the stone.

Standard optical microscopy was done on a Leica DMLP polarized light microscope. We used point counts to estimate volume percents of matrix, clasts, and melt glass, and the modal distribution of matrix minerals. We counted a total of 729 points over the entire ~920 mm$^2$ section for overall clast and matrix volumes. For additional point counts of the fine-grained matrix, six backscattered electron (BSE) images of optically "typical" areas of the matrix were counted on grids spaced at 10 $\mu$m intervals, giving a total of 2836 points over $2.914 \times 10^5$ $\mu$m$^2$. Modes of individual clasts were also determined from BSE images.

Chemical analysis, scanning electron microscope (SEM)-BSE imaging, and SEM x-ray mapping were done using a Cameca SX50 electron microprobe at the Lunar and Planetary Laboratory, University of Arizona. We calibrated the elements Mg, Si, Na, P, Al, Ca, K, Mn, Ti, Fe, Cr, and Ni with routine



Prelude preprint MS#4808

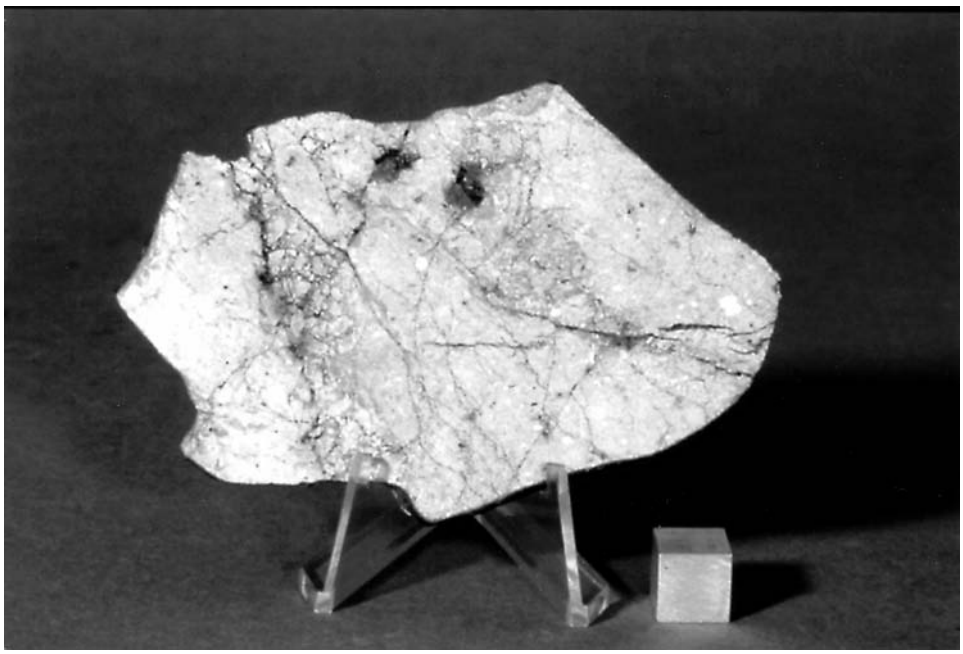

FIG. 1. A complete slab of NWA 482. Slightly darker matrix material surrounds lighter, mostly anorthositic clasts, in a clearly brecciated texture. Thin sections were chosen in order to sample the two pockets of dark melt glass visible at the top of the slice. For scale, the cube is 1 cm on each side.

standards, and then checked the calibration against olivine ($Fo_{83}$ and $Fo_{90}$), anorthite, and ilmenite standards. For analyses of silicate minerals, the beam was set to spot mode, at a voltage of 15 kV and a current of 15 nA. For analyses of the melt glass, the beam diameter was increased to 10 $\mu$m and the current was reduced to 10 nA to minimize sample volatility. The standards Yellowstone rhyolitic glass (USNM 72854) and synthetic tektite glass (USNM 2213) were checked to insure the glass was not overly volatilized by this setup. We set peak counting times to 20 s in all cases.

Samples for $^{40}Ar$-$^{39}Ar$ experiments were irradiated with neutrons at the University of Michigan reactor. They were then step-heated in a resistance-heated Ta furnace, with the evolved gas analyzed in the University of Arizona VG5400 noble gas mass spectrometer. The *J* factor for irradiation dose (McDougall and Harrison, 1999), $(8.55 \pm 0.09) \times 10^{-2}$, was determined by analysis of the MMhb-1 standard (Cohen *et al.*, 2002). The correction factor for Ca production at $^{39}Ar$, $^{39}Ar_{Ca}/^{37}Ar_{Ca} = (5.3 \pm 0.6) \times 10^{-4}$, was determined from analyses of samples of nakhlites that had been included in the same irradiation (Swindle and Olson, 2002), after $CaF_2$ samples included as monitors failed to give consistent results.

For $^{14}C$ measurements, we performed an initial pretreatment to remove weathering carbonates and evaporites. The sample (0.32 g) was crushed and treated with 85% $H_3PO_4$, washed with distilled water, and dried. The residue was mixed with ~3 g of iron chips (used to enhance combustion) and preheated in air at 500 °C for 1 h. Finally, the samples were loaded into a radio frequency (RF) induction furnace and heated in a flow of oxygen up to ~1700 °C. This process completely fused the rock powder and iron. The gases evolved were passed over $MnO_2$ and CuO/Pt (Jull *et al.*, 1993), collected at –196 °C, and then excess oxygen was removed under vacuum. Carbon dioxide was separated from water at –78 °C. The $CO_2$ volume was measured in a known volume using a capacitance manometer, and diluted to 1–2 $cm^3$ at STP with $^{14}C$-free $CO_2$. The gas was then reduced to graphite, which was subsequently pressed into an accelerator target, which was mounted in the accelerator ion source, along with standards of graphite prepared from National Institute of Standards and Technology (NIST) standards. From the isotope ratio of the graphite measured by accelerator mass spectrometry (AMS), the $^{14}C$ content of the meteorite in atoms/g (or dpm/kg) were calculated as discussed by Jull *et al.* (1998). Analyses were conducted at the NSF Arizona AMS laboratory at the University of Arizona.

## RESULTS

### Macroscopic Description

The whole rock had a smooth, dark brown crust, similar in appearance to a fusion crust. Visible clasts showed through

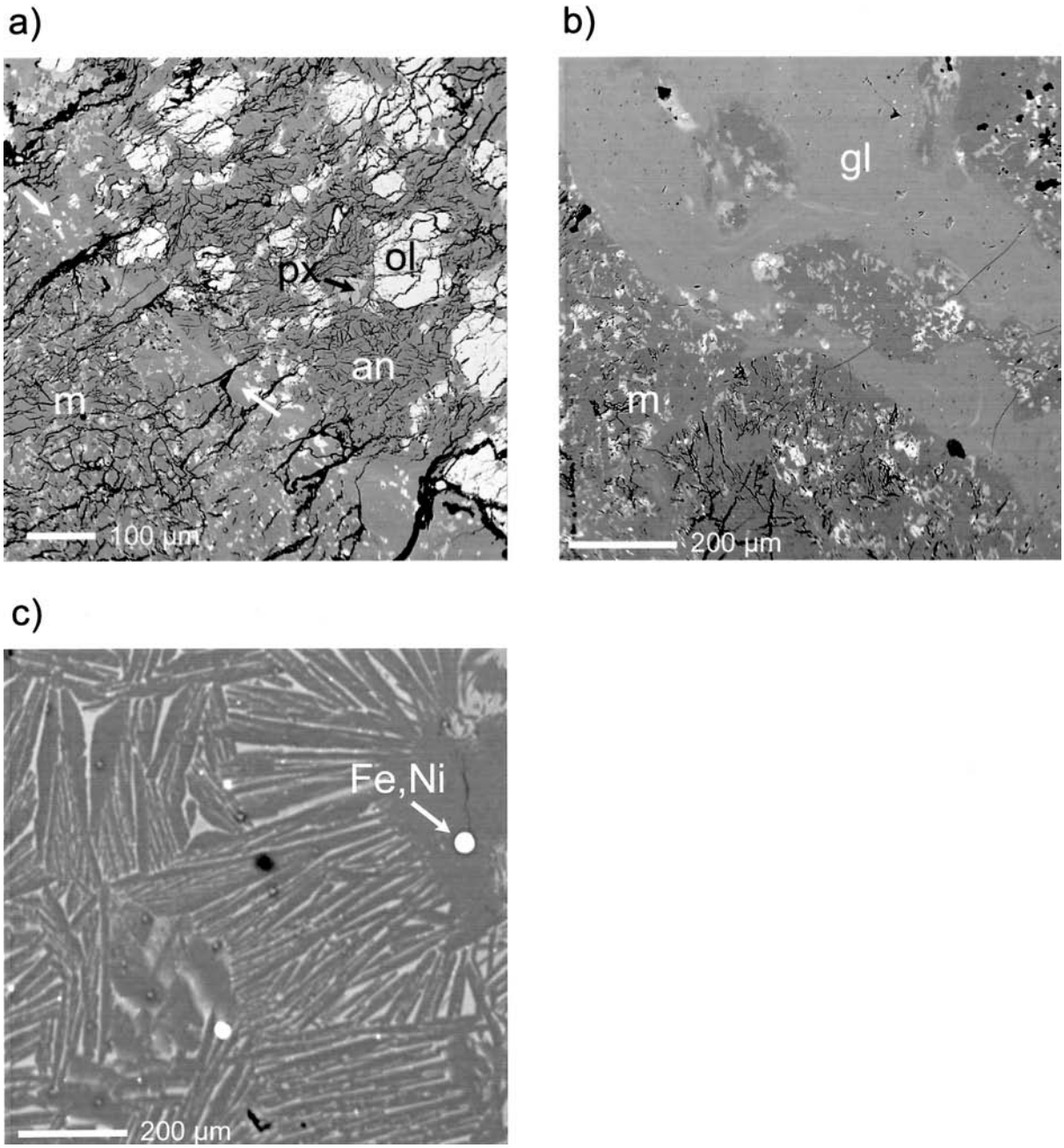


FIG. 2. Backscattered electron images of NWA 482. (a) A spinel troctolite clast (upper right) next to the fine-grained matrix (m) (lower left). The clast consists of olivine (ol), anorthitic plagioclase (an), and minor pyroxene (px). The clast also contains several small pleonaste spinels, which are not visible in this image. Smaller olivine and pyroxene (lighter gray), along with more anorthite (darker gray) make up the matrix. Between the matrix and the clast, there is a thin strip of glassy quench zone (between the white arrows). (b) One of the shock glass veins (gl) and surrounding matrix (m). Streaks of slightly different compositions within the glass outline the flow of the melt. "Islands" of unmelted matrix material are isolated in the middle of the vein; thin recrystallization bands surround them. An isolated plagioclase mineral clast is partially visible at the bottom of the image. (c) A recrystallized texture typical of the large pockets of melt glass. Blebs of Fe,Ni metal appear as white spots.

this outer layer, indicating that portions were covered with only a thin remnant fusion crust, or a layer caused by terrestrial alteration, such as desert varnish or ventifact polishing. Very little fusion crust existed in our thin section of the meteorite.

In the sliced hand sample (Fig. 1), the rock is obviously a breccia, with a fine-grained very light grey (N8; Rock-Color Chart Committee, 1991) matrix enclosing generally brighter, very light grey to white (N8-9) clasts. Cracks are visible throughout the rock, especially between matrix and clasts. Darker, light grey (N7) areas of apparently cataclasized material and dark grey (N3) vesicular impact melt veins and pockets crosscut the rock.

## Microscopic Description

In thin section the rock is dominated by an igneous-textured matrix surrounding mineral and lithic clasts. As described below, the clasts are shock-metamorphosed; there are also veins and pockets of glass running through the section. We interpret the overall texture of the rock to be that of a crystallized impact-melt breccia.

**Matrix**–Poikilitic matrix (Fig. 2a,b) represents 67 vol% of the original breccia (not including the areas which are cross-cut by glassy veins and melt pockets). It is holocrystalline and consists of tiny (a few to ~10 $\mu$m) subhedral to anhedral olivine (average $Fa_{33.5}$; 21 analyses) (Fig. 3), magnesium pigeonite to subcalcic augite (average $Wo_{14.9}En_{60.5}Fs_{24.6}$; 13 analyses), and augite (average $Wo_{35.4}En_{49.0}Fs_{15.6}$; 2 analyses) (Fig. 4), which are subophitically enclosing larger (~50 to 100 $\mu$m) euhedral to subhedral laths of anorthositic plagioclase feldspar (average $An_{95.8}Or_{0.16}Ab_{4.0}$; 47 analyses) (Table 1). The relative proportions of minerals vary locally, but average 85 vol% plagioclase, 5% olivine, and 10% pyroxene (2836 points). Matrix interstices were generally opaque. Trace Fe,Ni-metal and possible ilmenite are also present, but no phosphate or silica minerals were observed.

Matrix olivine and pyroxene have average Mg numbers (molar Mg/(Mg + Fe) × 100) of 66.55 ± 0.63 (21 analyses) and 71.75 ± 2.02 (15 analyses), respectively. The ratio of these values is 1.08, within the range of ratios for equilibrated olivines and pyroxenes, so the mafic minerals are in equilibrium, as expected for an impact melt that cooled slowly. These Mg

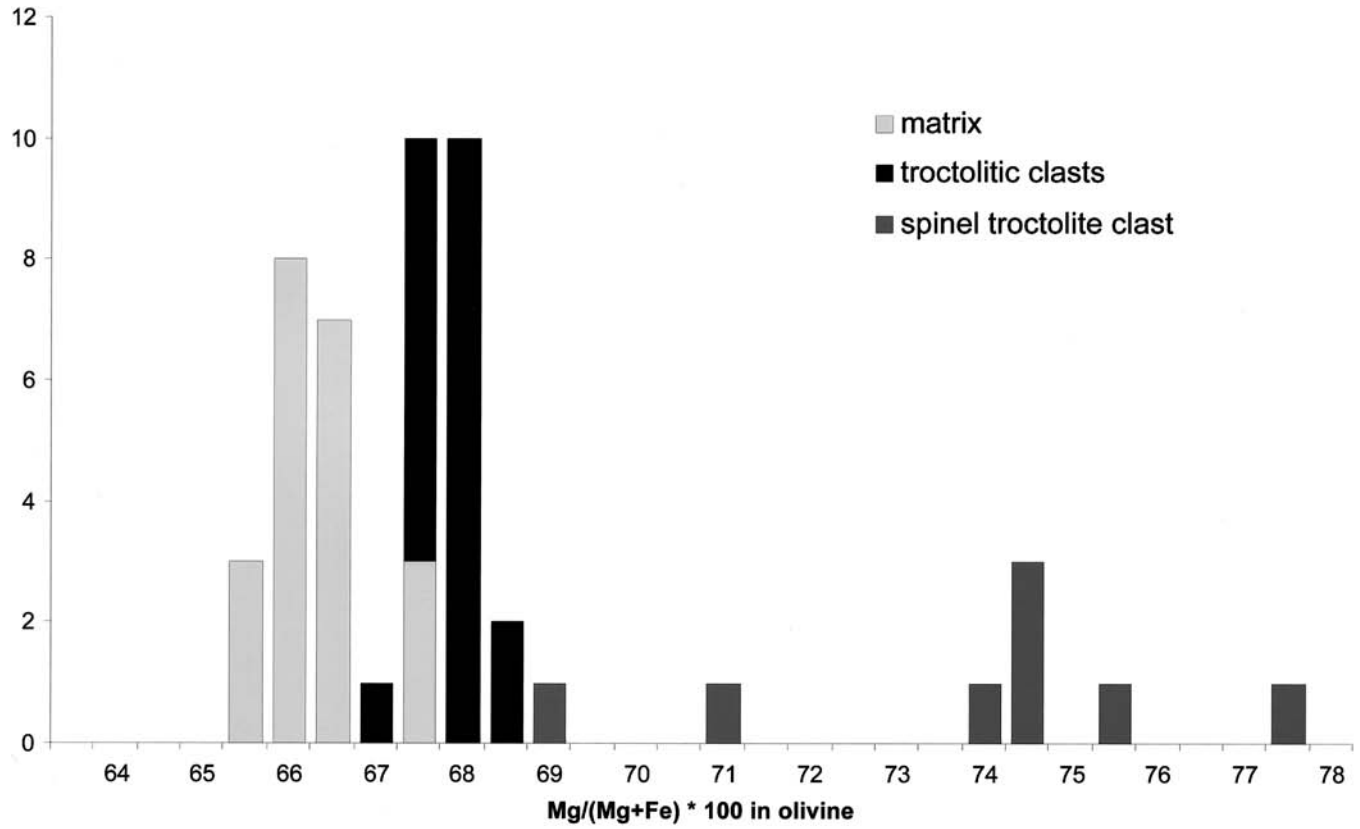


FIG. 3. Histogram of olivine Fo (molar Mg/(Mg + Fe) × 100) in NWA 482. Patterns differentiate olivines in the matrix and different types of clasts. Olivines in troctolitic clasts (including troctolites and anorthositic troctolites) are just slightly more magnesian than the matrix average of $Fo_{66.5}$. The spinel troctolite clast is significantly more magnesian and has a much wider compositional range; however, it is still not as magnesian as most spinel troctolites (see Fig. 6).

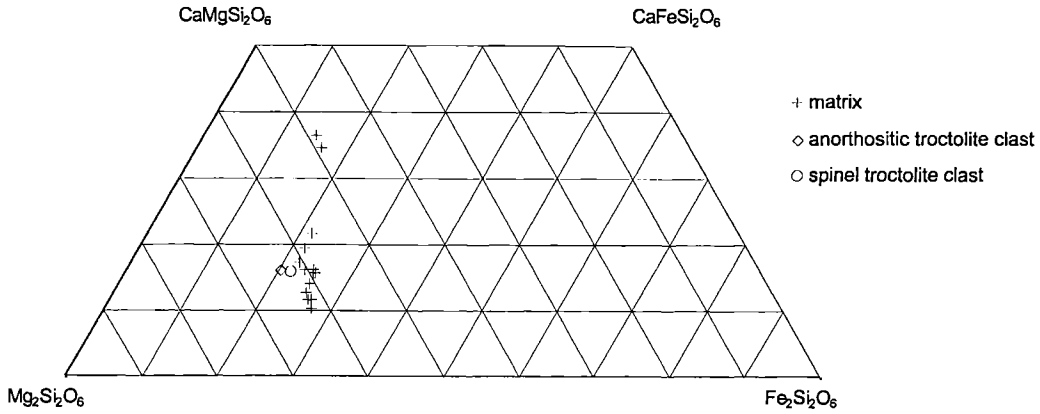


FIG. 4. Pyroxene quadrilateral for NWA 482. Matrix pyroxenes (+) seem to fall into two groups, moderate- and high-Ca (magnesium pigeonite to subcalcic augite, and augite, respectively). Clastic pyroxenes (open symbols) are rare, and have compositions only slightly more magnesian than the pigeonite seen in the matrix. Analytical uncertainties are smaller than symbols.

TABLE 1. Representative mineral compositions.

| | Plagioclase | | Pyroxene | | Olivine | | | Spinel | |
|---|---|---|---|---|---|---|---|---|---|
| wt% | Matrix | Anorthite clasts | Matrix | Matrix high Ca | Matrix | Troctolitic clasts | Spinel troctolite clast | Mineral clast | Spinel troctolite clast |
| $Na_2O$ | 0.45 | 0.46 | 0.03 | 0.07 | 0.01 | 0.00 | 0.01 | 0.00 | 0.00 |
| $P_2O_5$ | 0.03 | 0.04 | 0.03 | 0.04 | 0.02 | 0.01 | 0.00 | 0.00 | 0.00 |
| $K_2O$ | 0.03 | 0.02 | 0.00 | 0.00 | 0.00 | 0.00 | 0.00 | 0.00 | 0.00 |
| FeO | 0.30 | 0.10 | 14.5 | 10.0 | 29.4 | 28.4 | 23.0 | 15.1 | 16.6 |
| $SiO_2$ | 43.8 | 43.3 | 51.8 | 50.6 | 35.8 | 36.9 | 36.8 | 0.03 | 0.12 |
| MgO | 0.09 | 0.06 | 21.1 | 16.8 | 32.8 | 34.1 | 38.0 | 17.9 | 14.3 |
| CaO | 19.6 | 19.4 | 7.79 | 16.4 | 0.31 | 0.21 | 0.30 | 0.05 | 0.25 |
| NiO | 0.01 | 0.00 | 0.03 | 0.00 | 0.01 | 0.00 | 0.01 | 0.02 | 0.03 |
| $Cr_2O_3$ | 0.00 | 0.00 | 0.72 | 0.69 | 0.14 | 0.10 | 0.24 | 5.43 | 31.1 |
| $Al_2O_3$ | 36.4 | 36.5 | 2.06 | 2.89 | 0.09 | 0.06 | 0.37 | 63.9 | 38.4 |
| MnO | 0.02 | 0.00 | 0.31 | 0.23 | 0.30 | 0.30 | 0.29 | 0.15 | 0.37 |
| $TiO_2$ | 0.04 | 0.03 | 0.44 | 1.09 | 0.12 | 0.05 | 0.02 | 0.11 | 0.81 |
| Total | 100.80 | 99.91 | 98.81 | 98.75 | 99.06 | 100.17 | 99.04 | 102.69 | 101.98 |
| An | 95.85 | 95.80 | – | – | – | – | – | – | – |
| Or | 0.19 | 0.10 | – | – | – | – | – | – | – |
| Ab | 3.95 | 4.09 | – | – | – | – | – | – | – |
| Wo | – | – | 16.06 | 34.43 | – | – | – | – | – |
| En | – | – | 60.56 | 49.10 | – | – | – | – | – |
| Fs | – | – | 23.37 | 16.47 | – | – | – | – | – |
| *mg#* | – | – | 72.15 | 74.88 | 66.55 | 68.17 | 74.67 | – | – |

numbers are also within the range of other crystalline impact-melt breccias (*e.g.*, Papike *et al.*, 1991).

**Clasts**–Isolated mineral and lithic clasts of different types are embedded in the matrix, making the rock a polymict breccia. Mineral clasts are not as abundant as lithic clasts, volumetrically: isolated mineral clasts constitute ~26.8 vol% of the clastic material. The mineral clasts are anorthositic feldspars, with an average of $An_{95.7}Or_{0.14}Ab_{4.1}$ (43 analyses). There is very little variation in the feldspar compositions (Table 1), although there is a slightly larger spread in mole percent An in the clasts compared to the matrix feldspars. The feldspars are often twinned and heavily fractured (see below for discussion of shock effects); some have cataclastic textures. No pyroxene or olivine mineral clasts were observed.

One isolated mineral clast is a small (~100 × 200 $\mu$m) pleonaste spinel, appearing purple in plane-polarized light. It

is anhedral, with one fractured surface, and more fractures throughout the crystal. Its composition is $(Mg_{0.7}Fe_{0.3})(Al_{1.9}Cr_{0.1})O_4$ (4 analyses), with very little Ti (<0.04 atom%). This is more Mg- and Al-rich (Fe- and Cr-poor) than chromite spinels usually found in lunar rocks, even anorthositic ones (*e.g.*, Papike *et al.*, 1991; Jolliff and Haskin, 1995). The only lunar rocks observed to contain pleonaste are spinel troctolites (Fig. 5), therefore this mineral clast probably originated in a spinel troctolite rock.

Lithic clasts include igneous highland rocks from the ferroan anorthosite group, including anorthosites and troctolitic rocks. Like other lunar highlands meteorites, there is a lack of Mg-suite material (*e.g.*, Jolliff *et al.*, 1991). No mafic or potassium-, rare-earth-element-, and phosphorus-bearing (KREEP) lithologies were observed.

Some anorthosite clasts are quite large, with anorthite crystals up to millimeters across. They are also rich in Ca, with an average An indistinguishable from other feldspars, both matrix and clastic. Troctolite (2), anorthositic troctolite (6), and troctolitic anorthosite (1) clasts are present. The specific classification was determined by modal analysis of the clasts, using the definitions of Stöffler *et al.* (1980). Of course, the small sample sizes (the largest clast measured is <2 mm) may be biasing these modal classifications, but in most cases the grains are much smaller than the clasts. These clasts show large plagioclase crystals poikilitically enclosing anhedral olivine grains. Minor pyroxene is also present in most of them. One of the largest (~1440 × 1480 $\mu$m) of these, a troctolite (Fig. 2a), has a tiny Cr-rich pleonaste spinel ($(Mg_{0.6}Fe_{0.4})(Al_{1.3}Cr_{0.7})O_4$; 1 analysis) (Fig. 5), making that clast a spinel troctolite (actually an anorthositic spinel troctolite, using the classification of Stöffler *et al.*, 1980). This spinel is compositionally distinct from the lone spinel crystal discussed above—it is more Cr-rich, and slightly less magnesian. Olivine and pyroxene in this

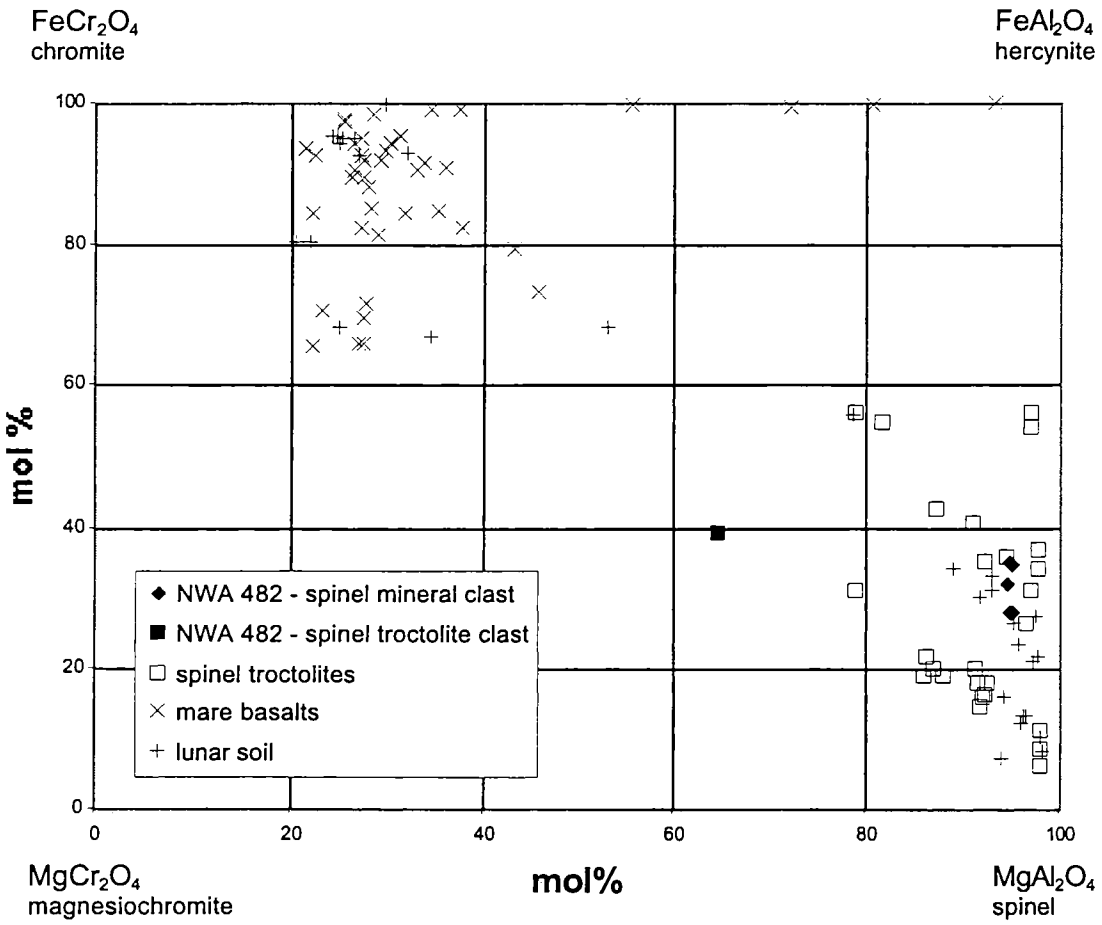


FIG. 5. Spinel compositions in NWA 482 (■ and ◆) compared to other lunar spinels. Pleonaste "pink" spinels found in NWA 482 are typical of those reported in other spinel troctolites (□), and well within the range of reported compositions. Spinels in mare basalts (×) are in general more Fe- and Cr-rich. Spinels found in lunar soil (+) are clearly from a variety of rock types, including spinel troctolites. Mare basalt and soil data from Papike *et al.* (1991); additional soil data from Jolliff and Haskin (1995) and Weiblen *et al.* (1974); spinel troctolite data from Baker and Herzberg (1980), Bence *et al.* (1974), Dymek *et al.* (1976), Marvin *et al.* (1989), Prinz *et al.* (1973), Ridley *et al.* (1973), Roedder and Weiblen (1977), and Snyder *et al.* (1998, 1999).

particular clast have nearly identical Mg numbers, 74.1 in both cases. Olivines in other troctolitic clasts are all ~$Fo_{68}$; with plagioclase ~$An_{96}$ (Fig. 6), these lithologies all have affinities to the ferroan anorthosite (FAN) suite.

Other ferroan troctolitic rocks have also been found among lunar samples. Lunar breccia 64435 includes a coarse-grained troctolitic anorthosite clast with similar mineralogy to the troctolitic anorthosite in NWA 482 (James *et al.*, 1989), although the olivine is slightly more magnesian ($Fo_{71.5}$ compared to $Fo_{67}$ in the NWA 482 clast). Warren and Wasson (1977) found another example of a troctolitic anorthosite, 62237, that falls in the ferroan anorthosite grouping of rocks (Fig. 6). The lunar meteorite MacAlpine Hills (MAC) 88104/5 also contains clasts of ferroan troctolitic anorthosites (Jolliff *et al.*, 1991; Warren and Kallemeyn, 1991). These clasts, "WX1" (Warren and Kallemeyn, 1991) and "W2" (Jolliff *et al.*, 1991), are additional examples of the few troctolitic samples like those in NWA 482 that are too ferroan to be considered part of the Mg-rich suite of highlands rocks (Warren, 1993). These troctolitic clasts are magnesian enough to be considered a part of the "mafic, magnesian" subgroup of the ferroan anorthosite suite described in James *et al.* (1989).

**Glass**–Our sample contains several dark veins and irregular pockets of glass, the largest of which are ~1.5 mm across. We found no beads of glass, glass shards, or agglutinates. The glass takes up ~11 vol% of the thin section studied (the area was chosen to include two large melt pockets). Flow of the glass is evinced by schlieren, which are visible in optical and BSE images (*e.g.*, Fig. 2b). Also, submicron opaque particles of metal and/or sulfides are disseminated through the melt glass, following flow lines. Some veins have incorporated "clasts" of the host matrix (*e.g.*, Fig. 2b). Large areas of the two main melt pockets are now devitrifying into spherical and radial growths of crystals (Fig. 2c).

The average composition of several veins and the two main pockets of glass is shown in Table 2. The average composition we measured is in good agreement with that measured by other workers (Warren and Kallemeyn, 2001). The glass is anorthositic, although some areas are more ferrous (maximum in one analysis 8.5 wt% FeO), due probably to the poor mixing of shock glass prior to quenching. This type of compositional variation is local, within veins and pockets; average compositions do not vary much *between* veins and pockets (Fig. 7). It is therefore likely that glass analyses are a reasonable estimate of the meteorite's bulk composition.

**Metal and sulfides**–We observed no metals or sulfides in hand sample, or without magnification on the thin section. High-magnification optical and electron microscopy revealed a very small amount of metal, in the form of irregular grains in the matrix and tiny blebs in the melt glass (Fig. 2c). Most are <10 $\mu$m across. The metal appears to be Fe,Ni-metal, although the grains are so small we could not perform analyses that were not contaminated by surrounding silicates.

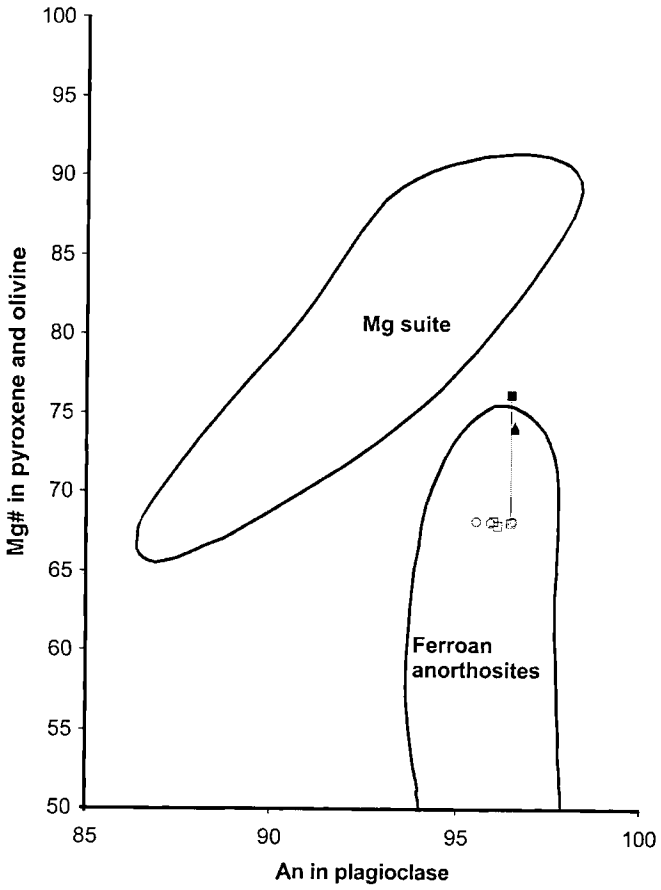


FIG. 6. Igneous clast mineralogy: An (molar Ca/(Ca + K + Na) × 100) in feldspars plotted *vs. mg#* (molar Mg/(Mg + Fe) × 100) in mafic minerals (olivine and pyroxene). Open symbols are olivine analyses, filled symbols are pyroxene analyses, and lines connect the two when both are from the same clast. In the case of the spinel troctolite (▲), pyroxene and olivine Mg numbers are so close as to be indistinguishable on this plot. Most troctolite clasts (○) and anorthositic troctolite clasts (□) lie in the ferroan anorthosite range. The most magnesian clasts observed are still less magnesian (more ferroan) than "Mg suite" rocks with the same An. The outlines of the two groups are based on Marvin *et al.* (1989) and Warren (1993).

## Alteration/Weathering

The outer edge of the stone appears to have a weathering rind, which is distinct from several remnants of a glassy fusion crust. X-ray maps show concentrations of K along cracks, which contrast with the very low amounts of K in most of the rock and the melt glass. The location and habit of the K indicates that it is the result of weathering. Although levels of $K_2O$ in the melt glass (Table 2; see also Warren and Kallemeyn, 2001) are low, indicating terrestrial alteration of the glass is minimal, it has undoubtedly affected the rock to some degree.

Where alteration has affected the rock, typically near the pockets and veins of melt glass, it has been altered to unidentified phyllosilicates and carbonates. Replacement

TABLE 2. Shock melt glass composition in NWA 482, compared to some other lunar meteorites.

| | NWA 482 | | DaG 400* | Dhofar 026† | Dhofar 301‡ | Dhofar 302‡ | Dhofar 303‡ |
|---|---|---|---|---|---|---|---|
| wt% | Shock melt glass, this study, 85 analyses | Shock melt glass, Warren and Kallemeyn (2001) | Bulk rock (broad beam) | Bulk rock | Impact-melt matrix | Impact-melt glassy matrix | Impact-melt matrix |
| $Na_2O$ | 0.41 | 0.4 | 0.33 | 0.24 | 0.39 | 0.41 | 0.34 |
| $P_2O_5$ | 0.04 | – | – | 0.05 | 0.07 | 0.12 | 0.03 |
| $K_2O$ | 0.02 | 0.03 | 0.1 | 0.08 | 0.04 | 0.09 | 0.01 |
| FeO | 2.82 | 3.5 | 3.52 | 4.06 | 4.27 | 4.02 | 3.2 |
| $SiO_2$ | 43.7 | 44.6 | 43.4 | 44.31 | 44.1 | 44.5 | 44.0 |
| MgO | 3.15 | 3.6 | 3.8 | 3.92 | 4.83 | 4.84 | 4.97 |
| CaO | 17.6 | 17.5 | 18.68 | 16.99 | 16.5 | 16.5 | 16.9 |
| NiO | 0.03 | – | – | – | – | – | – |
| $Cr_2O_3$ | 0.06 | 0.07 | 0.3 | 0.08 | 0.10 | 0.09 | 0.06 |
| $Al_2O_3$ | 31.4 | 29.2 | 29.16 | 29.59 | 28.6 | 28.1 | 29.7 |
| MnO | 0.04 | – | 0.06 | 0.06 | 0.07 | 0.06 | 0.06 |
| $TiO_2$ | 0.13 | 0.13 | 0.23 | 0.22 | 0.36 | 0.27 | 0.15 |
| Total | 99.43 | 99.03 | 99.58 | 99.61 | 99.33 | 99.00 | 99.42 |
| *mg#*§ | 66.6 | 64.7$ | 65.8$ | 63.2$ | 66.8$ | 68.2 | 73.5 |

*Semenova *et al.* (2000).
†Taylor *et al.* (2001).
‡Nazarov *et al.* (2002).
§*mg#* = atomic Mg/(Mg + Fe) × 100.
$Calculated from oxides, assuming all Fe in $Fe^{+2}$.

minerals are present in several glass veins. Limonitic staining and rusty orange-brown staining, typical of Fe-oxide mobilization, is visible in many areas, again especially noticeable near the glass and along the edge of the section that corresponds to the outer surface of the rock.

## Shock Classification

We used the shock classification method of Stöffler *et al.* (1991). Although this method is specifically for ordinary chondrites, the method should still be fairly accurate for this rock, as it is based on shock effects in olivine and plagioclase, and on whole-rock effects. The original formation of the breccia would have required a shock level of greater than ~75 GPa for the melting that produced the matrix. The presence of many crosscutting, interconnected melt pockets and veins indicates a later shock event of level S4 (moderately shocked) or higher; this indicates a pressure of >30 GPa, but less than ~75 GPa, was reached in portions of the rock.

A detailed study of the shock level of the clasts was not possible due either to the small size of most clasts, or the small sizes of the crystals within them. Most of the clasts are individual plagioclase crystals or lithic anorthosites, and these all show undulose extinction and irregular fractures, although none are isotropic or maskelynitized. They therefore have experienced shock of level S2–S3 (very weakly to weakly shocked, about 5–20 GPa).

One large spinel troctolite clast (Fig. 2a) is large enough for the type of detailed study outlined in Stöffler *et al.* (1991). We selected 10 olivine crystals at least 50 $\mu$m across at random and examined them for shock effects. They show undulose extinction, irregular fractures, and most of them have parallel planar fractures, but no mosaicism or planar deformation features. We studied plagioclase crystals in the same manner. They are irregularly fractured with undulose extinction, but are not isotropic or maskelynitized, and none have planar deformation features. Although the plagioclase indicates a shock level similar to that of the anorthositic clasts, the olivine indicates a higher shock level of S3–S4 (weakly to moderately shocked, about 30–35 GPa).

## Argon-40–Argon-39 Ages

Results of our $^{40}Ar$-$^{39}Ar$ age determination are summarized in Table 3. The bulk sample contained nearly twice as much of both $^{40}Ar$ and $^{39}Ar$ as the glass sample. The difference was predominantly at the lower temperatures, the bulk sample releasing more than 3× as much $^{39}Ar$ by the 1100 °C step.

Apparent ages are not corrected for $^{40}Ar$ from either (terrestrial) atmospheric argon or from (lunar) trapped Ar. Since

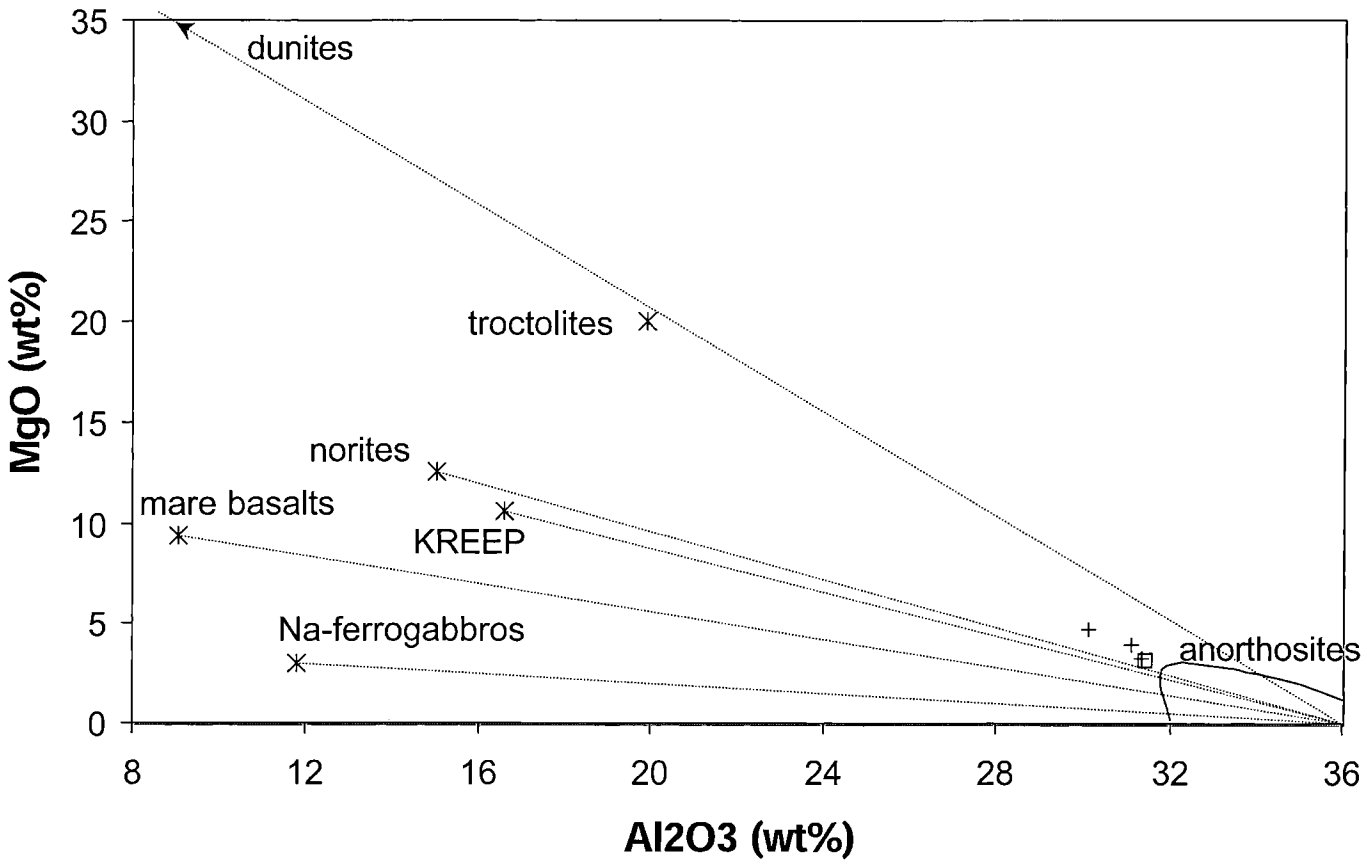


FIG. 7. On a plot of wt% $Al_2O_3$ *vs.* MgO, the shock glass lies near a bulk mixing line between anorthosites and Mg-rich rocks (troctolites, norites, dunites). The compositions of the shock glass differ only slightly between three different melt pockets (+). The average of all melt pockets and melt veins (□) is closest to the composition of the largest melt pocket. This is a reflection of the observed clast population, which is dominated by anorthosites, but also includes some troctolitic clasts. Troctolites did not constitute a large volume of the rock, and were low in MgO (Fig. 6). This may explain the low weight percent MgO in the glass compared to a typical troctolite–anorthosite mixing line. Alternatively, there may be a lower-Mg rock type (*e.g.*, norite) incorporated into the glass, which is not present in the remaining clast population. Although the KREEP mixing line also appears to lie near NWA 482 glasses on this plot, no KREEP component was observed (*e.g.*, very low weight percent $K_2O$, $P_2O_5$; Table 2). Plot after Stöffler *et al.* (1985); data from Taylor *et al.* (1991).

the $^{36}Ar/^{40}Ar$ ratios (Table 3) are almost all greater than or equal to the atmospheric value of 0.0034, an atmospheric correction would remove all of the $^{40}Ar$ in almost every case. Although samples were baked to ~200 °C overnight before analysis to drive off adsorbed gas, the $^{36}Ar/^{40}Ar$ ratio is virtually identical to the atmospheric value at the lowest temperatures for each sample. We believe that this $^{40}Ar$ is probably dominated by terrestrial contamination.

It is plausible that there could have been some lunar Ar trapped (other than incompletely degassed radiogenic Ar from the sample itself). The most likely source would be Ar trapped through interaction with the solar wind. This would be expected to have a $^{40}Ar/^{36}Ar$ ratio of 1 to 10, depending on time of entrapment (Eugster *et al.*, 2001). We can test for this several ways. First, three-isotope plots (not shown) give no hint of an isochron or a unique trapped component. Next, we can look at $^{36}Ar/^{38}Ar$ ratios. Except for the extractions dominated by terrestrial contamination, this ratio is always 0.65 or lower. Ratios of ~0.6 are typical of cosmic-ray spallation for lunar rocks (Hohenberg *et al.*, 1978), while solar wind or terrestrial components have ratios of >5 (lower ratios can be caused by $^{38}Ar$ created by neutron capture on Cl). In addition, the total amount of $^{36}Ar$, other than that which we have attributed to terrestrial contamination, is nearly the same in the two samples, $2.32 \times 10^{-7}$ cm$^3$ STP/g for the bulk *vs.* $2.45 \times 10^{-7}$ cm$^3$ STP/g for the glass, which we would not necessarily expect for incorporation of solar wind and other trapped Ar, but would expect for spallation. If $^{36}Ar$ is dominated by spallation, then any lunar trapped component is likely to be an insignificant correction to $^{40}Ar$. Hence we see no evidence for any nonradiogenic $^{40}Ar$, except for those extractions at the lowest and highest temperatures with terrestrial contamination.

The bulk sample does not give an age plateau (Fig. 8). Instead, there is a pattern of generally increasing apparent ages with increasing extraction temperature, except for two notable excursions to much lower apparent ages, each time associated

TABLE 3. Argon in irradiated NWA 482.

| Temp. (°C) | $^{39}Ar_K$ ($10^{-9}$ cm$^3$ STP/g) | $^{39}Ar_K/^{37}Ar_{Ca}$ | $^{36}Ar/^{40}Ar$ | Apparent age (Ma)* |
|---|---|---|---|---|
| | | **Bulk** (6.399 mg) | | |
| 300 | 3.4 | 0.033 | 0.0035 | 9670 ± 24 |
| 400 | 4.3 | 0.029 | 0.0035 | 8127 ± 21 |
| 450 | 3.3 | 0.028 | 0.0036 | 6256 ± 22 |
| 500 | 6.3 | 0.039 | 0.0061 | 2143 ± 21 |
| 600 | 30.5 | 0.050 | 0.0109 | 855 ± 10 |
| 700 | 6.5 | 0.0082 | 0.0166 | 2312 ± 22 |
| 800 | 10.5 | 0.0058 | 0.0194 | 2771 ± 22 |
| 900 | 19.6 | 0.0044 | 0.0212 | 3173 ± 26 |
| 1000 | 18.0 | 0.0039 | 0.0210 | 3333 ± 28 |
| 1050 | 8.6 | 0.0046 | 0.0241 | 3016 ± 25 |
| 1100 | 28.1 | 0.0132 | 0.0200 | 1816 ± 14 |
| 1150 | 12.0 | 0.0045 | 0.0228 | 3103 ± 25 |
| 1200 | 16.8 | 0.0038 | 0.0249 | 3313 ± 29 |
| 1250 | 6.2 | 0.0034 | 0.0230 | 3531 ± 33 |
| 1300 | 5.6 | 0.0037 | 0.0200 | 3638 ± 31 |
| 1350 | 4.9 | 0.0036 | 0.0197 | 3722 ± 33 |
| 1400 | 8.8 | 0.0036 | 0.0191 | 3774 ± 32 |
| 1450 | 5.2 | 0.15 | 0.0198 | 3736 ± 18 |
| 1500 | 0.1 | –† | 0.0040 | 8560 ± 630 |
| Total | 198.7 | | | |
| | | **Glass** (2.875 mg) | | |
| 300 | 1.5 | 0.132 | 0.0034 | 9905 ± 56 |
| 400 | 2.3 | 0.027 | 0.0033 | 7388 ± 49 |
| 500 | 1.1 | 0.0047 | 0.0031 | 4006 ± 47 |
| 700 | 4.3 | 0.0207 | 0.0071 | 2804 ± 34 |
| 900 | 12.6 | 0.0174 | 0.0104 | 2358 ± 21 |
| 1100 | 23.6 | 0.0076 | 0.0224 | 2407 ± 19 |
| 1300 | 22.8 | 0.0029 | 0.0231 | 3794 ± 37 |
| 1400 | 40.6 | 0.0026 | 0.0263 | 3713 ± 40 |
| 1550 | 0.2 | 0.0025 | 0.0108 | 5708 ± 94 |
| Total | 109.0 | | | |

*Uncertainties in ages are 1$\sigma$, and include uncertainty in $J$ factor.
†Blank levels of $^{37}Ar$.

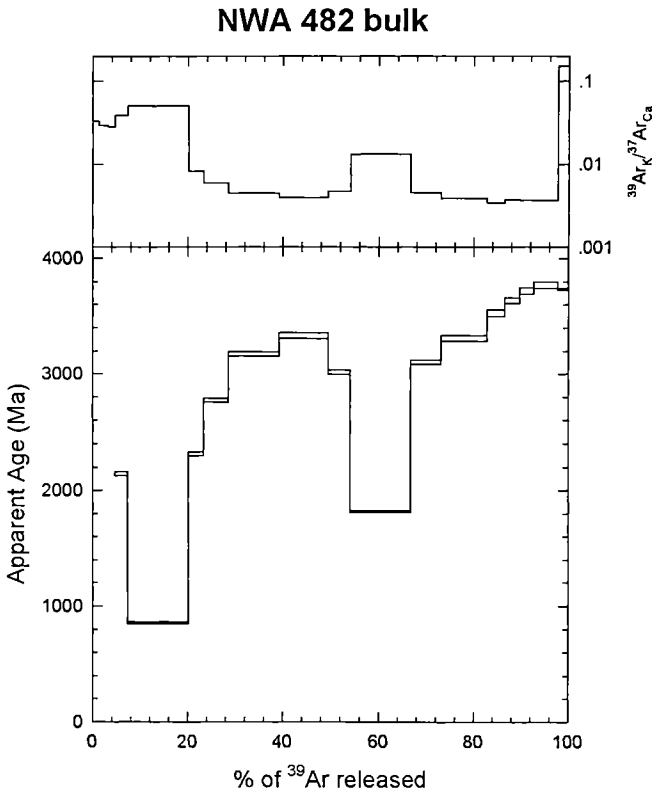


FIG. 8. Plot of $^{39}Ar_K/^{39}Ar_{Ca}$ (top) and apparent $^{40}Ar/^{39}Ar$ age (bottom) as a function of the fraction of the K-derived $^{39}Ar$ released, for the sample of bulk NWA 482. Note that $^{39}Ar_K/^{39}Ar_{Ca}$ is directly proportional to the K/Ca ratio in the mineral that is outgassing in that temperature step. Difficulty with the Ca irradiation monitor (discussed in text) makes it impossible to precisely define the conversion factor, but note that the major minerals, plagioclase and pyroxene, have average K/Ca ratios of 0.0012 and 0.0017, respectively. Size of the boxes in lower panels represent 1$\sigma$ uncertainties.

with very high K/Ca ratios. Since the first excursion actually follows a series of steps with K/Ca values that are almost as high, it could either represent (a) the true age of a low-temperature high-K phase, with the higher ages preceding it an artifact of terrestrial $^{40}Ar$ contamination or (b) a contaminant terrestrial phase. The low apparent age in the 1100 °C step is surrounded by releases with higher apparent ages and lower K/Ca ratios. We believe this is likely to be a contaminant with very high K and a very low age—if 60% of the $^{39}Ar$ in the extraction were contributed by something with a zero age, it would explain the result, and the K/Ca is roughly 3× as high as in adjacent steps. Our suspicion that the low apparent ages are terrestrial contaminants is strengthened by the high concentrations of K located along cracks, where terrestrial weathering would be most expected.

Hence, we interpret the bulk of the data as being released from pyroxene and plagioclase (both with comparably low K/Ca ratios), showing evidence of a thermal event strong enough to cause significant loss of $^{40}Ar$, but not strong enough to completely reset the system. The highest ages, at the highest temperatures, represent a lower limit to the age of the rock before that event. The 1450 °C step, with a higher K/Ca but an age similar to the two preceding steps, is plausibly olivine, which is rare, but has a much higher K/Ca ratio on average (note: the representative mineral analyses in Table 1 were chosen for their major element concentrations and their stoichiometry, not necessarily for minor elements such as K and Ca in olivine). The 1350, 1400, and 1450 °C steps all give ages of 3700 to 3800 Ma and can be summed to give an average age of ~3740 Ma.

The analysis of the glass is consistent with this interpretation (Fig. 9). As mentioned above, little gas was released until the 1300 °C step. It and the 1400 °C step gave an amount equal to

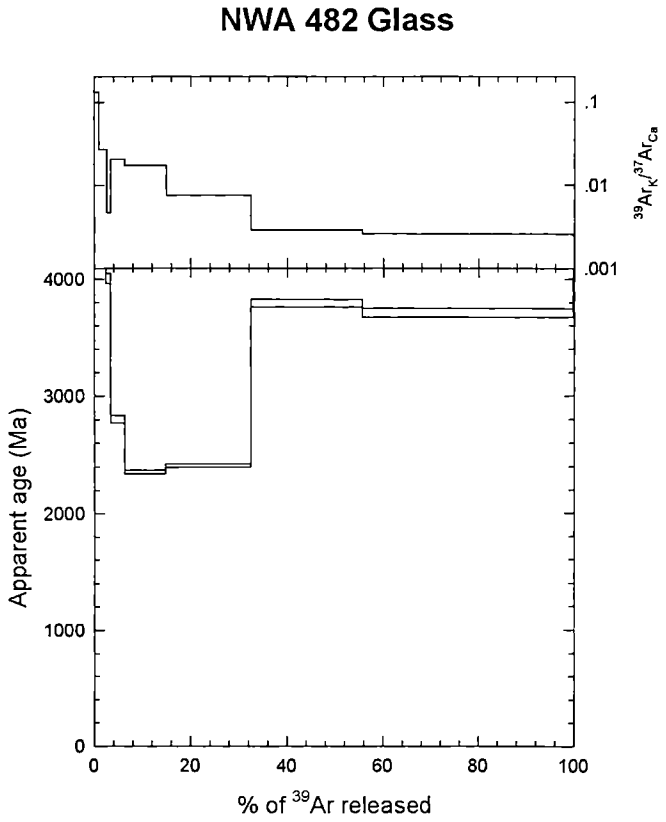


FIG. 9. Plot of $^{39}Ar_K/^{39}Ar_{Ca}$ (top) and apparent $^{40}Ar/^{39}Ar$ age (bottom) as a function of the fraction of the K-derived $^{39}Ar$ released, for the sample of shock glass in NWA 482. See Fig. 8 for more details.

less than a third of the total in the bulk sample, but amounting to 68% of the $^{39}Ar_K$ in the glass. They both give apparent ages of between 3700 and 3800 Ma (averaging ~3750 Ma), with a K/Ca ratio comparable to most of the releases from the bulk sample.

### Carbon-14 Age

Based on $^{14}C$ measurements, NWA 482 has a terrestrial age of 8.6 ± 1.3 ka (Table 4; Fig. 10). This terrestrial age is consistent with the amount of weathering seen in the rock (see description above).

A previous measurement of the terrestrial age for this meteorite (Nishiizumi and Caffee, 2001a) was much longer then this (60–120 ka). However, based on additional $^{41}Ca$ data, this value was revised downwards to ~15 ka by the authors (K. Nishiizumi, pers. comm.).

## DISCUSSION

### Lunar Provenance

The highly anorthositic nature of NWA 482 is the strongest evidence that it is lunar. Terrestrial anorthosites are rare, and most have mole percent An in the range about 40–80, with only a few Archean anorthosites having mole percent An up to 90 (Ashwal, 1988).

TABLE 4. $^{14}C$ measurements and terrestrial age.

| | | |
|---|---|---|
| $^{14}C$ | 23.1 ± 0.5 dpm/kg | |
| Saturated activity | 65 dpm/kg | Jull *et al.* (1998) |
| Terrestrial age | | |
| $^{14}C$ | 8.6 ± 1.3 ka | |
| $^{36}Cl$ | 60–120 ka | Nishiizumi and Caffee (2001a) |
| $^{41}Ca/^{36}Cl$ | ~15 ka | Nishiizumi (pers. comm) |

A commonly used indicator of planetary derivation is the elemental ratio Fe/Mn in bulk rocks and/or in mafic minerals; however, the range of values in this rock is too large to be conclusive on this point. Olivines had an average Fe/Mn of 92.50 ± 7.75 (clasts and matrix did not vary too much on average; compare 92.32 for clastic olivines and 93.17 for olivines in matrix). The spread in Fe/Mn values is fairly large, though, ranging from ~70 to 110. Pyroxenes had a much lower average Fe/Mn of 48.96 ± 11.96, again with a broad range. However, this spread in Fe/Mn is typical of lunar olivines and pyroxenes, and is bracketed by the range of values seen in other lunar crystalline impact-melt breccias (*e.g.*, 65–160 for olivines, 32–84 for pyroxenes; Papike *et al.*, 1991). The average of pyroxene and olivine analyses gives an average Fe/Mn of 79 ± 22, which is close to the average of ~70 for Apollo samples (Wänke *et al.*, 1975; Palme *et al.*, 1991).

### Impact History

This rock has a fairly complex history. Clasts of igneous anorthositic and troctolitic rocks may represent remainders of parent lithologies. All of the precursor rocks most likely were igneous highlands material, because no remnants of regolith material remain (glass shards, agglutinates, *etc.*). If any regolith was included, the textures have been destroyed by melting of the matrix.

Clasts of primary igneous rocks were incorporated into the rock when, at one point, the entire matrix was melted and then recrystallized around the clasts. In order for the melted matrix to cool slowly enough to form the texture observed, this impact must have been fairly large. Deutsch and Stöffler (1987) estimated that in order to produce subophitic melt rocks (like NWA 482), an impact crater would have to be larger than ~5 km in diameter. Craters smaller than this do not produce enough melt to insulate the center of the melt sheet and slow cooling rates to those measured for rocks like these. Clasts remained unmelted, but might have been weakly to moderately shocked at this point. Even an impact which produces a crater 5 km across can easily create the shock levels recorded in this rock (*e.g.*, French, 1998). The impact event that created the NWA 482 impact-melt breccia could have been either a simple crater or a complex crater (lunar transition diameter ~15 km; Melosh, 1989).

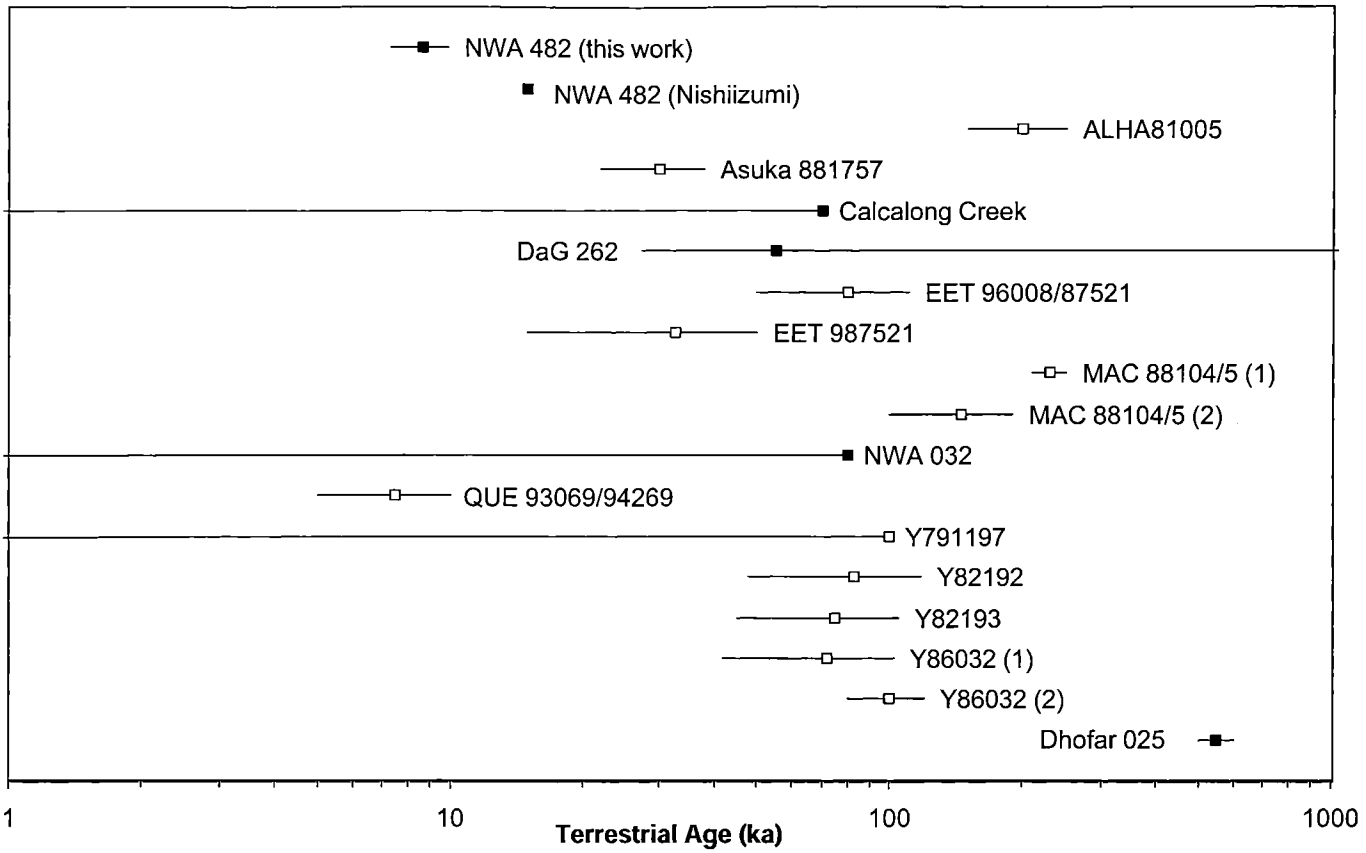


FIG. 10. Terrestrial exposure ages for Antarctic lunar meteorites (□) and lunar meteorites found in hot deserts (■). NWA 482 is one of the youngest, and apparently unpaired, although this does not rule out a source-crater pairing. NWA 482 = this work, and Nishiizumi (pers. comm.); ALHA81005 = Nishiizumi *et al.* (1989); Asuka 881757 = Thalmann and Eugster (1994); Calcalong Creek = Nishiizumi *et al.* (1992); DaG 262 = Nishiizumi *et al.* (1998); EET 96008/87521 = Nishiizumi *et al.* (1999); EET 987521 = Vogt *et al.* (1993); MAC 88104/5 = Nishiizumi *et al.* (1991) (1), and Vogt *et al.* (1991) (2); NWA 032 = Nishiizumi and Caffee (2001b); QUE 93069/94269 = Nishiizumi *et al.* (1996); Y-791197 = Vogt *et al.* (1991); Y-82192 and Y-82193 = Eugster and Niedermann (1988); Y-86032 = Eugster (1989) (1) and Vogt *et al.* (1991) (2); Dhofar 025 = Nishiizumi and Caffee (2001a).

At some later time another shock event produced the melt glass that now cuts across the rock in veins and large pockets; the shock recorded in the clasts might also have occurred during this event. An impact event also lifted the rock off the surface of the Moon; this could be the same event that created the melt glass, but more likely it is a third impact event. The launch is too recent: even when the stone's ~9 ka terrestrial stay is subtracted from the youngest age recorded in the meteorite (~2400 Ma), typical Moon–Earth transit times for lunar meteorites are much shorter. Transit times are less than ~10 Ma (Warren, 1994) (or perhaps even shorter: most are <15 ka according to Benoit *et al.*, 1996). Therefore the younger age cannot represent the meteorite's ejection.

The rock's tumultuous history probably erased the older igneous ages of the highland clasts from the $^{40}$Ar-$^{39}$Ar system. Instead, we see two dominant ages that may represent two of the above impact events, or possibly another thermal event that was not recorded in the petrology. We believe the most plausible interpretation is that the event that formed the impact-melt breccia occurred <3750 Ma ago, completely resetting the K-Ar system in the rock. A subsequent thermal event, perhaps the formation of the glass veins, caused substantial, but not complete, $^{40}$Ar loss no more than ~2400 Ma ago. An alternative interpretation is that the glassy veins and melt pockets formed at ~3750 Ma, and that lower apparent ages represent another event that is not recorded petrographically.

The oldest ages seen in this rock are younger than most pristine ferroan anorthosites. Samarium-Nd ages, which are less susceptible to impact resetting, show much older ages in the range about 4.4–4.5 Ga (Taylor *et al.*, 1991; Borg *et al.*, 1999; Stöffler and Ryder, 2001). Even most $^{40}$Ar-$^{39}$Ar ages of FANs are older than NWA 482; although they do range at least from 3.63 to 4.23 Ga (Schaeffer *et al.*, 1976; Borg *et al.*, 1999; Norman *et al.*, 2000), these ages often represent impact resetting similar to that in NWA 482, rather than original crystallization ages. The ages measured for NWA 482 therefore do not correspond to any anorthosite clasts that might have been unaltered prior to the lithification of the impact-melt breccia, which appears to have completely reset the K-Ar system.

NWA 482 is also younger than the majority of highland impact melts, most of which fall ~3.9 Ga (Dalrymple and Ryder, 1993; Taylor *et al.*, 1991; Stöffler and Ryder, 2001); however there are some impact-melt breccias from Apollo, which have similar ages (*e.g.*, crystalline impact-melt breccia 76055 has a coincident age of 3.78 ± 0.04 Ga; Tera *et al.*, 1974). Most of the large impact basins that have been dated are also older—Nectaris, Serenitatis, and Crisium basins all being dated between 3.89 and 3.9 Ga (Stöffler and Ryder, 2001; Ryder *et al.*, 2000). Younger craters that have been dated, such as Autolycus, Copernicus, Tycho, North and South Ray Craters, and Cone Crater, are all much younger than the ~3.75 and 2.4 Ga ages recorded in NWA 482 (Stöffler and Ryder, 2001). Imbrium basin is probably 3.75–3.85 Ga old (Deutsch and Stöffler, 1987; Stadermann *et al.*, 1991; Dalrymple and Ryder, 1993; Ryder *et al.*, 2000; Stöffler and Ryder, 2001); the lower limit corresponds closely to the age of NWA 482. Orientale basin has not been dated with radiometric analyses of impact lithologies, but has been estimated to be as old as 3.84 Ga, and perhaps as young as 3.72 Ga, which is the age of lava flows which postdate the impact (*e.g.*, Stöffler and Ryder, 2001). This lower limit is also fairly close to the 3.75 Ga age of NWA 482.

Based on the uncertainties among basin ages on the near side, the NWA 482 impact-melt breccia was either formed near the end of the basin-forming impact events or shortly thereafter. If it was produced after the basin-forming events, it may have occurred during a period of moderately high impact flux, hints of which also appear among howardite–eucrite–diogenite group meteorites (HEDs) (Bogard, 1995) as well as other lunar impact ages (Cohen, 2000; Cohen *et al.*, 2000; Culler *et al.*, 2000).

Normative calculations were done using the Cross, Iddings, Pirsson and Washington (CIPW) method (after Cox *et al.*, 1979). The composition of the shock-melted glass corresponds to a normative plagioclase abundance of 89.6% by volume, compared to a marginally lower value of 84.8 vol% for the matrix, according to point counts. Using the classification method of Stöffler *et al.* (1980) for lunar highland rocks, the matrix composition corresponds to that of a gabbroic anorthosite, while the shock melt glass has a composition closer to, but not quite, anorthosite (≥90% plagioclase). We interpret this to be the result of simply mixing the (more gabbroic) matrix with (dominantly anorthitic) clasts to produce a glass that contains more anorthite than the matrix. When the rock was shock melted, both clasts and matrix would have been incorporated into the melt in roughly the proportions we see in the remaining unmelted rock. If we assume all the clastic material is plagioclase (not a bad assumption, since the mineral clasts are almost all plagioclase, and only a few troctolitic rocks were found among the lithic clast population), then combining the clasts and matrix in the proportions we observe gives 89.8 vol% plagioclase, almost exactly the normative amount in the shock glass.

The matrix may be more mafic than the bulk rock (represented by the shock glass) because pyroxenes and olivines were preferentially melted when the breccia was created. Differences in the compositions of the matrix and the clast population were also observed in Apollo 17 melt breccias (Simonds, 1975; Dymek *et al.*, 1976; Ryder *et al.*, 1997). This discrepancy may be because the shock impedance is greater between mafic phases and plagioclase than between adjacent plagioclase crystals. Alternatively, it may imply different source areas for the matrix and clasts. However, the difference in composition is so small that errors involved in the above calculation, mostly stemming from the point count of the matrix, are just as likely the cause of the discrepancy.

### A Sample of the Far Side?

Although the specific locality of a meteorite's origin is nearly impossible to decipher due to the randomness of meteorite impacts, the absence of typical mare and KREEP components suggest a far side highlands provenance for NWA 482.

The melt glass is highly anorthositic, with more than 31 wt% $Al_2O_3$ (Table 2; see also Warren and Kallemeyn, 2001). This is higher than most Apollo impact melts and melt rocks (*e.g.*, Vaniman and Papike, 1980; Stöffler *et al.*, 1985; Taylor *et al.*, 1991) and the global average for highlands crust (Warren and Kallemeyn, 1991). The molar Ca/Al ratio has been used in combination with $TiO_2$ content to distinguish mare and highland rocks (*e.g.*, Wood, 1975; Warren and Kallemeyn, 1991). The ratio Ca/Al in the melt glass averages 0.511 ± 0.02, only slightly above that for stoichiometric anorthite. Combined with the <0.13 wt% $TiO_2$ in the melt glass (Table 2; also Warren and Kallemeyn, 2001), this material is clearly of highlands origin. In several areas of the matrix, a few tiny needles, ~10 μm long and <1 μm across (too small for uncontaminated microprobe analyses), were found to have roughly equal amounts of Ti and Fe, and therefore are probably ilmenite. This is the only example of titanite minerals seen in the thin section. The compositions of the glass and matrix support the lack of visual evidence for any surviving basaltic clasts. As far as we can tell, any clastic mare contribution is nonexistent.

Incompatible elements also seem to be present in strikingly low concentrations. No phosphorus or potassium minerals were found; if they exist in this sample, they are rare and small. Shock glasses had <0.08 and 0.05 wt% $P_2O_5$ and $K_2O$, respectively. We examined x-ray maps of a large area of the crystalline matrix and a smaller area at high magnification, specifically looking for P- and K-bearing phases, which might have been missed. None were found. Levels of P and K are very low, except for a slight concentration of K along cracks, discussed above, which appears to be a result of terrestrial weathering.

Texturally, NWA 482 resembles some of the "subophitic-ophitic-intersertal melt breccias" of Stöffler *et al.* (1985) and the compositional "group 4" of Korotev (1994). Although there is a lot of compositional variety in those rocks, the glass composition of NWA 482 is close to the average composition of the group (Korotev 1994). NWA 482 is also chemically

similar to individual feldspathic breccias from the Apollo collection (Taylor *et al.*, 1991). For example, crystalline impact-melt breccias such as 15445 (Ridley *et al.*, 1973), 67475 (Lindstrom *et al.*, 1977), and 67559 (Stöffler *et al.*, 1985) all have comparable major element concentrations. However, these other rocks usually have textural or chemical properties which differentiate them from NWA 482: for example, clastic fragments of KREEP-enriched rocks, a KREEP component in the melt matrix, and/or a contribution from mare basalts (Marvin *et al.*, 1987; Stöffler *et al.*, 1985). Sample 67559 is also significantly older than NWA 482 (Stöffler *et al.*, 1985). Although the composition of NWA 482 is grossly similar to that of the fragmental breccia 67015 (Wänke *et al.*, 1975), the fragmental textures in 67015 are distinct.

Not only are lunar maria concentrated on the near side of the Moon, KREEP rocks are also confined to regions on the near side, according to thorium abundances measured by the *Lunar Prospector* (Lawrence *et al.*, 1998). The source of KREEP is believed to be the last vestiges of incompatible elements to solidify from a primordial magma ocean. While many soils and breccias are enriched in KREEP, igneous rocks with the KREEP pattern are limited mainly to Apollo 15 KREEP basalts. These rocks are temporally and spatially related to the Imbrium impact event (Ryder, 1994; Papike *et al.*, 1998), and are possibly a result of impact-induced volcanism (Ryder, 1994). This limits the possible origin of a rock lacking any KREEP component to either someplace far from the Imbrium impact (*e.g.*, the far side), or a period in the Moon's history before that impact occurred. Finding ages older than Imbrium in NWA 482 that have not been reset by more recent impacts would strengthen, although not confirm, the second possibility. Since NWA 482 does not have any ages that precede Imbrium, it likely formed on the far side.

### An Unpaired Lunar Meteorite?

NWA 482 appears to be unique; it is not paired with any known lunar meteorite. Although several other lunar meteorites resemble NWA 482 in bulk composition (Table 2) and in the observed clast populations, none of them are the same texturally. NWA 482 has no regolith component, no glass spheres or shards, and no KREEP, mare, or Mg-suite lithologies.

The short terrestrial age rules out most pairing possibilities (Fig. 10). Only Queen Alexandra Range (QUE) 93069/94269 has a similar terrestrial age (Nishiizumi *et al.*, 1996), but it is both Antarctic and a regolith breccia, so cannot be paired with NWA 482. Although some lunar meteorites only have upper limits on their terrestrial ages (Fig. 10), they each differ from NWA 482 in either their place of terrestrial origin or rock type, or both. Of course, the possibility of a source-crater pairing (Warren, 1994) might still remain.

Although impact-melt breccias comprise about 30–50% of returned highland rocks (Hörz *et al.*, 1991) and are the most abundant rock type at the Apollo 16 landing site (Korotev, 1994), few lunar meteorites have been classified as such. Other highland impact-melt breccias include Dhofar 026, Dar al Gani (DaG) 400, and several new Dhofar meteorites. These meteorites have bulk compositions similar to the shock-melted glass in NWA 482 (Table 2), and none of them have published terrestrial ages that would rule out a pairing.

Dhofar 026 is a crystalline impact-melt breccia (Cohen *et al.*, 2001), but is unlike NWA 482 in other ways. Dhofar 026 is more clast-poor, and includes basaltic melt spherules, which are absent in NWA 482. The cosmogenic nuclide concentrations in the two meteorites are also very different (Nishiizumi and Caffee, 2001a). Finally, the crystallization age of Dhofar 026 (~500 Ma; Cohen *et al.*, 2002) is much younger than any of the ages recorded in NWA 482.

The Dar al Gani meteorites are possible pairs since, like NWA 482, they are also from the Sahara. Although most literature classifies DaG 400 as a regolith breccia (*e.g.*, Zipfel *et al.*, 1998), one abstract refers to it as an impact-melt breccia (Bukovanska *et al.*, 1999). Having examined this meteorite in thick section and BSE images, we do not believe it is an impact-melt breccia. Since it is a regolith breccia, it probably cannot be paired with NWA 482.

Several new lunar meteorites, Dhofar 301, 302, 303, and 489, have recently been discovered in Oman (Nazarov *et al.*, 2002; Russell *et al.*, 2002). Preliminary work on these stones indicate they represent distinct impact-melt breccias with highland affinities. Dhofar 301 contains a very low titanium (VLT) basalt clast, and Dhofar 302 contains fragments of KREEP glass, making these two unlikely pairs for NWA 482. On the other hand, not enough is known about Dhofar 303 and 489 to determine whether they could be paired with NWA 482. Dhofar 303 is free of either mare or KREEP components, and the mineralogy and chemistry are similar to those of NWA 482. Dhofar 489 has only recently been announced in the *Meteoritical Bulletin* (Russell *et al.*, 2002), and its description seems inconsistent, calling it both a fragmental breccia and a crystalline matrix breccia. More work needs to be done on these stones to determine the likelihood of a pairing with NWA 482.

## CONCLUSIONS

NWA 482 is a crystalline impact-melt breccia from the highlands of the Moon, probably the far side. Precursor target rocks were mostly anorthosites and troctolites. Regolith contributions, if there were any, were absorbed into the breccia matrix and their textures destroyed. Very little, if any, mare or KREEP material was incorporated into the breccia. A separate shock event created veins and pockets of melt glass, the anorthositic composition of which reflects that of the bulk rock. Radiometric $^{40}Ar$-$^{39}Ar$ ages indicate two events, one at ~3750 Ma, which was either the lithification of the breccia, or the later formation of the shock glass; and a more recent event

at ~2400 Ma, which could also date of the formation of the shock glass, or some later thermal event. A short terrestrial age, combined with the unique lithology of NWA 482, preclude any pairings with other lunar meteorites, with the possible exception of the newly-discovered Dhofar 303 and 489.

*Acknowledgments*–The authors would like to thank M. Farmer for donating the sample of NWA 482 and B. A. Cohen for her assistance with the noble gas analyses. Ken Domanik was very helpful, as always, with the microprobe. Marc Norman and Otto Eugster provided extremely helpful reviews, and Randy Korotev was an invaluable editor. We also thank Alan Rubin and Paul Warren, who provided much of the data used by the Meteorite Nomenclature Committee to classify the sample as a lunar meteorite. This work was supported by the University of Arizona (I. J. D. and D. A. K.), NASA Cosmochemistry Grant NAG5-4767 (T. S.), and NASA grant NAG5-4832 (A. J. T. J.).

*Editorial handling:* R. Korotev

## REFERENCES

ASHWAL L. D. (1988) Anorthosites: Classification, mythology, trivia, and a simple unified theory. In *Workshop on the Deep Continental Crust of South India* (ed. L. D. Ashwal), pp. 30–32. LPI Technical Report **88-06**, Lunar and Planetary Institute, Houston, Texas, USA.

BAKER M. B. AND HERZBERG C. T. (1980) Spinel cataclasites in 15445 and 72435: Petrology and criteria for equilibrium. *Proc. Lunar Planet. Sci. Conf.* **11th**, 535–553.

BENCE A. E., DELANO J. W., PAPIKE J. J. AND CAMERON K. L. (1974) Petrology of the highlands massifs at Taurus-Littrow: An analysis of the 2–4 mm soil fraction. *Proc. Lunar Planet. Sci. Conf.* **5th**, 785–827.

BENOIT P. H., SEARS D. W. G. AND SYMES S. J. K. (1996) The thermal and radiation exposure history of lunar meteorites. *Meteorit. Planet. Sci.* **31**, 869–875.

BOGARD D. D. (1995) Impact ages of meteorites: A synthesis. *Meteoritics* **30**, 244–268.

BORG L., NORMAN M., NYQUIST L., BOGARD D., SNYDER G., TAYLOR L. AND LINDSTROM M. (1999) Isotopic studies of ferroan anorthosite 62236: A young lunar crustal rock from a light rare-earth-element-depleted source. *Geochim. Cosmochim. Acta* **63**, 2679–2691.

BUKOVANSKA M., DOBOSI G., BRANDSTÄTTER F. AND KURAT G. (1999) Dar al Gani 400: Petrology and geochemistry of some major lithologies (abstract). *Meteorit. Planet. Sci.* **34 (Suppl.)**, A21.

COHEN B. A. (2000) Geochemistry and $^{40}$Ar-$^{39}$Ar geochronology of lunar meteorite impact melt clasts. Ph.D. thesis, Univ. Arizona, Tucson, Arizona, USA. 174 pp.

COHEN B. A., SWINDLE T. D. AND KRING D. A. (2000) Support for the lunar cataclysm hypothesis from lunar meteorite impact melt ages. *Science* **290**, 1754–1756.

COHEN B. A., TAYLOR L. A. AND NAZAROV M. A. (2001) Lunar meteorite Dhofar 026: A second-generation impact melt (abstract). *Lunar Planet. Sci.* **32**, #1404, Lunar and Planetary Institute, Houston, Texas, USA (CD-ROM).

COHEN B. A., SWINDLE T. D., TAYLOR L. A. AND NAZAROV M. A. (2002) $^{40}$Ar-$^{39}$Ar ages from impact melt clasts in lunar meteorites Dhofar 025 and Dhofar 026 (abstract). *Lunar Planet. Sci.* **23**, #1252, Lunar and Planetary Institute, Houston, Texas, USA (CD-ROM).

COX K. G., BELL J. D. AND PANKHURST R. J. (1979) *The Interpretation of Igneous Rocks*. George Allen and Unwin Publishers, London, U.K. 450 pp.

CULLER T. S., BECKER T. A., MULLER R. A. AND RENNE P. R. (2000) Lunar impact history from $^{40}$Ar/$^{39}$Ar dating of glass spherules. *Science* **287**, 1785–1788.

DALRYMPLE G. B. AND RYDER G. (1993) $^{40}$Ar/$^{39}$Ar age spectra of Apollo 15 impact melt rocks by laser step-heating and their bearing on the history of lunar basin formation. *J. Geophys. Res.* **98**, 13 085–13 095.

DEUTSCH A. AND STÖFFLER D. (1987) Rb-Sr-analyses of Apollo 16 melt rocks and a new age estimate for the Imbrium basin: Lunar basin chronology and the early heavy bombardment of the Moon. *Geochim. Cosmochim. Acta* **51**, 1951–1964.

DYMEK R. F., ALBEE A. L. AND CHODOS A. A. (1976) Petrology and origin of boulders #2 and #3, Apollo 17 Station 2. *Proc. Lunar Planet. Sci. Conf.* **7th**, 2335–2378.

EUGSTER O. (1989) History of meteorites from the Moon collected in Antarctica. *Science* **245**, 1197–1202.

EUGSTER O. AND NIEDERMANN S. (1988) Noble gases in lunar meteorites Yamato-82192 and -82193 and history of the meteorites from the Moon. *Earth Planet. Sci. Lett.* **89**, 15–27.

EUGSTER O., TERRIBILINI D., POLNAU E. AND KRAMERS J. (2001) The antiquity indicator argon-40/argon-36 for lunar surface samples calibrated by uranium-235-xenon-136 dating. *Meteorit. Planet. Sci.* **36**, 1097–1115.

FRENCH B. M. (1998) *Traces of Catastrophe: A Handbook of Shock-Metamorphic Effects in Terrestrial Meteorite Impact Structures*. LPI contribution No. **954**, Lunar and Planetary Institute, Houston, Texas, USA. 120 pp.

GROSSMAN J. N. AND ZIPFEL J. (2001) The Meteoritical Bulletin, No. 85, 2001 September. *Meteorit. Planet. Sci.* **36 (Suppl.)**, A293–A322.

HOHENBERG C. M., MARTI K., PODOSEK F. A., REEDY R. C. AND SHIRCK J. R. (1978) Comparisons between observed and predicted cosmogenic noble gases in lunar samples. *Proc. Lunar Planet. Sci. Conf.* **9th**, 2311–2344.

HÖRZ F., GRIEVE R., HEIKEN G., SPUDIS P. AND BINDER A. (1991) Lunar surface processes. In *Lunar Sourcebook: A User's Guide to the Moon* (eds. G. Heiken, D. Vaniman and B. M. French), pp. 61–120. Cambridge Univ. Press, New York, New York, USA.

JAMES O. B., LINDSTROM M. M. AND FLOHR M. K. (1989) Ferroan anorthosite from lunar breccia 64435—Implications for the origin and history of lunar ferroan anorthosites. *Proc. Lunar Planet. Sci. Conf.* **19th**, 219–243.

JOLLIFF B. L. AND HASKIN L. A. (1995) Cogenetic rock fragments from a lunar soil: Evidence of a ferroan noritic-anorthosite pluton on the Moon. *Geochim. Cosmochim. Acta* **59**, 2345–2374.

JOLLIFF B. L., KOROTEV R. L. AND HASKIN L. A. (1991) A ferroan region of the lunar highlands as recorded in meteorites MAC 88104 and MAC 88105. *Geochim. Cosmochim. Acta* **55**, 3051–3071.

JULL A. J. T., DONAHUE D. J., CIELASZYK E. AND WLOTZKA F. (1993) Carbon-14 terrestrial ages and weathering of 27 meteorites from the southern high plains and adjacent areas (USA). *Meteoritics* **28**, 188–195.

JULL A. J. T., CLOUDT S. AND CIELASZYK E. (1998) $^{14}$C terrestrial ages of meteorites from Victoria Land, Antarctica and the infall rates of meteorites. In *Meteorites: Flux with Time and Impact Effects* (eds. M. M. Grady, R. Hutchison, G. J. H. McCall and D. A. Rothery), pp. 75–91. Geological Society of London, Spec. Pub. **140**, London, U.K.

KOROTEV R. L. (1994) Compositional variation in Apollo 16 impact-melt breccias and inferences for the geology and bombardment history of the Central Highlands of the Moon. *Geochim. Cosmochim. Acta* **58**, 3931–3969.

LAWRENCE D. J., FELDMAN W. C., BARRACLOUGH B. L., BINDER A. B., ELPHIC R. C., MAURICE S. AND THOMSEN D. R. (1998) Global elemental maps of the Moon: The Lunar Prospector gamma-ray spectrometer. *Science* **281**, 1484–1489.

MARVIN U. B., LINDSTROM M. M., BERNATOWICZ T. J., PODOSEK F. A. AND SUGIURA N. (1987) The composition and history of breccia 67015 from North Ray Crater. *J. Geophys. Res.* **92**, E471–E490.

MARVIN U. B., MARVIN J., CAREY W. AND LINDSTROM M. M. (1989) Cordierite-spinel troctolite, a new magnesium-rich lithology from the lunar highlands. *Science* **243**, 925–928.

MCDOUGALL I. AND HARRISON T. M. (1999) *Geochronology and Thermochronology by the $^{40}Ar/^{39}Ar$ Method* (2nd edition). Oxford Univ. Press, New York, New York, USA. 269 pp.

MELOSH H. J. (1989) *Impact Cratering: A Geologic Process*. Oxford Univ. Press, New York, New York, USA. 245 pp.

MELOSH H. J. (1995) Cratering dynamics and the delivery of meteorites to Earth. *Meteoritics* **30**, 545–546.

NAZAROV M. A., DEMIDOVA S. I., PATCHEN A. AND TAYLOR L. A. (2002) Dhofar 301, 302, and 303: Three new lunar highland meteorites from Oman (abstract). *Lunar Planet. Sci.* **33**, #1293, Lunar and Planetary Institute, Houston, Texas, USA (CD-ROM).

NORMAN M., NYQUIST L., BOGARD D., BORG L., WEISMANN H., GARRISON D., YOUNG R., SHIH C-Y. AND SCHWANDT C. (2000) Age and origin of the highlands crust of the Moon: Isotopic and petrologic studies of a ferroan noritic anorthosite clast from Descartes breccia 67215 (abstract). *Lunar Planet. Sci.* **31**, #1552, Lunar and Planetary Institute, Houston, Texas, USA (CD-ROM).

NISHIIZUMI K. AND CAFFEE M. W. (2001a) Exposure histories of lunar meteorites Dhofar 025, 026 and Northwest Africa 482 (abstract). *Meteorit. Planet. Sci.* **36 (Suppl.)**, A148.

NISHIIZUMI K. AND CAFFEE M. W. (2001b) Exposure histories of lunar meteorites Northwest Africa 032 and Dhofar 081 (abstract). *Lunar Planet. Sci.* **32**, #2101, Lunar and Planetary Institute, Houston, Texas, USA (CD-ROM).

NISHIIZUMI K., ELMORE D. AND KUBIK P. W. (1989) Update on terrestrial ages of Antarctic meteorites. *Earth Planet. Sci. Lett.* **93**, 299–313.

NISHIIZUMI K., ARNOLD J. R., KLEIN J., FINK D., MIDDLETON R., KUBIK P. W., SHARMA P., ELMORE D. AND REEDY R. C. (1991) Exposure histories of lunar meteorites: ALHA81005, MAC 88104, MAC 88105, and Y-791197. *Geochim. Cosmochim. Acta* **55**, 3149–3155.

NISHIIZUMI K., ARNOLD J. R., CAFFEE M. W., FINKEL R. C. AND SOUTHON J. (1992) Exposure histories of Calcalong Creek and LEW 88516 meteorites (abstract). *Meteoritics* **27**, 270.

NISHIIZUMI K., CAFFEE M. W., JULL A. J. T. AND REEDY R. C. (1996) Exposure histories of lunar meteorites Queen Alexandra Range 93069 and 94269. *Meteorit. Planet. Sci.* **31**, 893–896.

NISHIIZUMI K., CAFFEE M. W. AND JULL A. J. T. (1998) Exposure histories of Dar al Gani 262 lunar meteorites (abstract). *Lunar Planet. Sci.* **29**, #1957, Lunar and Planetary Institute, Houston, Texas, USA (CD-ROM).

NISHIIZUMI K., MASARIK J., CAFFEE M. W. AND JULL A. J. T. (1999) Exposure histories of pair lunar meteorites EET 96008 and EET 87521 (abstract). *Lunar Planet. Sci.* **30**, #1980, Lunar and Planetary Institute, Houston, Texas, USA (CD-ROM).

PALME H., SPETTEL B., JOCHUM K. P., DREIBUS G., WEBER H., WECKWORTH G., WÄNKE H., BISCHOFF A. AND STÖFFLER D. (1991) Lunar highlands meteorites and the composition of the lunar crust. *Geochim. Cosmochim. Acta* **55**, 3105–3122.

PAPIKE J., TAYLOR L. AND SIMON S. (1991) Lunar minerals. In *Lunar Sourcebook: A User's Guide to the Moon* (eds. G. Heiken, D. Vaniman and B. M. French), pp. 183–284. Cambridge Univ. Press, New York, New York, USA.

PAPIKE J. J., RYDER G. AND SHEARER C. K. (1998) Lunar samples. In *Planetary Materials* (ed. J. J. Papike), pp. 5–1 to 5–234. Mineral. Soc. America, Washington, D.C., USA.

PRINZ M., DOWTY E., KEIL K. AND BUNCH T. E. (1973) Spinel troctolite and anorthosite in Apollo 16 samples. *Science* **179**, 74–76.

RIDLEY W. I., HUBBARD N. J., RHODES J. M., WEISMANN H. AND BANSAL B. (1973) The petrology of lunar breccia 15445 and petrogenetic implications. *J. Geol.* **81**, 621–631.

ROCK-COLOR CHART COMMITTEE (1991) *The Rock Color Chart*. Geological Society of America, Boulder, Colorado, USA.

ROEDDER E. AND WEIBLEN P. W. (1977) Barred olivine "chondrules" in lunar spinel troctolite 62295. *Proc. Lunar Sci. Conf.* **8th**, 2641–2654.

RUSSELL S. S., ZIPFEL J., GROSSMAN J. N. AND GRADY M. M. (2002) The Meteoritical Bulletin, No. 86, 2002 July. *Meteorit. Planet. Sci.* **37 (Suppl.)**, A157–A184.

RYDER G. (1994) Coincidence in time of the Imbrium basin impact and Apollo 15 KREEP volcanic flows: The case for impact-induced melting. In *Large Meteorite Impacts and Planetary Evolution* (eds. B. O. Dressler, R. A. F. Grieve and V. L. Sharpton), pp. 11–18. Geological Society of America Special Paper **293**, Geological Society of America, Boulder, Colorado, USA.

RYDER G., NORMAN M. D. AND TAYLOR G. J. (1997) The complex stratigraphy of the highland crust in the Serenitatis region of the Moon inferred from mineral fragment chemistry. *Geochim. Cosmochim. Acta* **61**, 1083–1105.

RYDER G., KOEBERL C. AND MOJZSIS S. J. (2000) Heavy bombardment of the Earth at ~3.85 Ga: The search for petrographic and geochemical evidence. In *Origin of the Earth and Moon* (eds. R. M. Canup and K. Righter), pp. 475–492. Univ. Arizona Press, Tucson, Arizona, USA.

SCHAEFFER O. A., HUSAIN L. AND SCHAEFFER G. A. (1976) Ages of highland rocks: The chronology of lunar basin formation revisited. *Proc. Lunar Sci. Conf.* **7th**, 2067–2092.

SEMENOVA A. S., NAZAROV M. A., KONONKOVA N. N., PATCHEN A. AND TAYLOR L. A. (2000) Mineral chemistry of lunar meteorite Dar al Gani 400 (abstract). *Lunar Planet. Sci.* **31**, #1252, Lunar and Planetary Institute, Houston, Texas, USA (CD-ROM).

SIMONDS C. H. (1975) Thermal regimes in impact melts and the petrology of the Apollo 17 Station 6 boulder. *Proc. Lunar Planet. Sci. Conf.* **6th**, 641–672.

SNYDER G. A., RUZICKA A., TAYLOR L. A. AND PATCHEN A. D. (1998) Journey to the center of the regolith: A spinel troctolite and other clasts from drive tube 68001 (abstract). *Lunar Planet. Sci.* **29**, #1144, Lunar and Planetary Institute, Houston, Texas, USA (CD-ROM).

SNYDER G. A., TAYLOR L. A., PATCHEN A., NAZAROV M. A. AND SEMENOVA T. S. (1999) Mineralogy and petrology of a primitive spinel troctolite and gabbros from Luna 20, eastern highlands of the Moon (abstract). *Lunar Planet. Sci.* **30**, #1491, Lunar and Planetary Institute, Houston, Texas, USA (CD-ROM).

STADERMANN F. J., HEUSSER E., JESSBERGER E. K., LINGNER S. AND STÖFFLER D. (1991) The case for a younger Imbrium basin: New $^{40}Ar$-$^{39}Ar$ ages of Apollo 14 rocks. *Geochim. Cosmochim. Acta* **55**, 2339–2349.

STÖFFLER D. AND RYDER G. (2001) Stratigraphy and isotope ages of lunar geologic units: Chronological standard for the inner solar system. *Space Sci. Rev.* **96**, 9–54.

STÖFFLER D., KNÖLL H-D., MARVIN U. B., SIMONDS C. H. AND WARREN P. H. (1980) Recommended classification and nomenclature of lunar highland rocks—A committee report. In *Proc. Conf. Lunar Highlands Crust* (eds. J. J. Papike and R. B. Merrill), pp. 51–70. Pergamon Press, New York, New York, USA.

STÖFFLER D. *ET AL.* (1985) Composition and evolution of the lunar crust in the Descartes Highlands, Apollo 16. *Proc. Lunar Planet. Sci. Conf.* **15th**, C449–C506.

STÖFFLER D., KEIL K. AND SCOTT E. R. D. (1991) Shock metamorphism of ordinary chondrites. *Geochim. Cosmochim. Acta* **55**, 3845–3867.

SWINDLE T. D. AND OLSON E. K. (2002) The timing of aqueous weathering on Mars: Clues from argon-40-argon-39 analyses of

whole-rock samples of the nakhlites Nakhla and Lafayette (abstract). *Meteorit. Planet. Sci.* **37 (Suppl.)**, A138.

TAYLOR G. J., WARREN P. H., RYDER G., DELANO J., PIETERS C. AND LOFGREN G. (1991) Lunar rocks. In *Lunar Sourcebook: A User's Guide to the Moon* (eds. G. Heiken, D. Vaniman and B. M. French), pp. 183–284. Cambridge Univ. Press, New York, New York, USA.

TAYLOR L. A., NAZAROV M. A., COHEN B. A., WARREN P. H., BARSUKOVA L. D., CLAYTON R. N. AND MAYEDA T. K. (2001) Bulk chemistry and oxygen isotopic compositions of lunar meteorites Dhofar 025 and Dhofar 026 (abstract). *Lunar Planet. Sci.* **32**, #1985, Lunar and Planetary Institute, Houston, Texas, USA (CD-ROM).

TERA F., PAPANASTASSIOU D. A. AND WASSERBURG G. J. (1974) Isotopic evidence for a terminal lunar cataclysm. *Earth Planet. Sci. Lett.* **21**, 1–21.

THALMANN CH. AND EUGSTER O. (1994) Cosmic ray exposure history of two basaltic lunar meteorites: Asuka 881757 and Yamato 793169 (abstract). *Meteoritics* **29**, 540.

VANIMAN D. T. AND PAPIKE J. J. (1980) Lunar highland melt rocks: Chemistry, petrology and silicate mineralogy. In *Proceedings of the Conference on the Lunar Highlands Crust* (eds. J. J. Papike and R. B. Merrill), pp. 271–337. Pergamon Press, New York, New York, USA.

VOGT S., FINK D., KLEIN J., MIDDLETON R., DOCKHORN B., KORSCHINEK G., NOLTE E. AND HERZOG G. F. (1991) Exposure histories of the lunar meteorites: MAC 88104, MAC 88105, Y-791197, and Y-86032. *Geochim. Cosmochim. Acta* **55**, 3157–3165.

VOGT S., HERZOG G. F., EUGSTER O., MICHEL TH., NIEDERMANN S., KRÄHENBÜHL U., MIDDLETON R., DEZFOULY-ARJOMANDY B., FINK D. AND KLEIN J. (1993) Exposure history of the lunar meteorite, Elephant Moraine 87521. *Geochim. Cosmochim. Acta* **57**, 3793–3799.

WÄNKE H., PALME H., BADDENHAUSEN H., DREIBUS G., JAGOUTZ E., KRUSE H., PALME C., SPETTEL B., TESCHKE F. AND THACKER R. (1975) New data on the chemistry of lunar samples: Primary matter in the lunar highlands and the bulk composition of the Moon. *Proc. Lunar Planet. Sci. Conf.* **6th**, 1313–1340.

WARREN P. H. (1993) A concise compilation of petrologic information on possibly pristine nonmare Moon rocks. *Am. Mineral.* **78**, 360–376.

WARREN P. H. (1994) Lunar and martian meteorite delivery services. *Icarus* **111**, 338–363.

WARREN P. H. AND KALLEMEYN G. W. (1991) The MacAlpine Hills lunar meteorite and implications of the lunar meteorites collectively for the composition and origin of the Moon. *Geochim. Cosmochim. Acta* **55**, 3123–3138.

WARREN P. H. AND KALLEMEYN G. W. (2001) New lunar meteorite Northwest Africa 482: An anorthositic impact-melt breccia with low KREEP content (abstract). *Meteorit. Planet. Sci.* **36 (Suppl.)**, A220.

WARREN P. H. AND WASSON J. T. (1977) Pristine nonmare rocks and the nature of the lunar crust. *Proc. Lunar Planet. Sci. Conf.* **8th**, 2215–2235.

WEIBLEN P. W., POWELL B. N. AND AITKEN F. K. (1974) Spinel-bearing feldspathic-lithic fragments in Apollo 16 and 17 soil samples: Clues to processes of early lunar crustal evolution. *Proc. Lunar Planet. Sci. Conf.* **5th**, 749–767.

WOOD J. A. (1975) Lunar petrogenesis in a well-stirred magma ocean. *Proc. Lunar Sci. Conf.* **6th**, 1087–1102.

ZIPFEL J., SPETTEL B., PALME H., WOLF D., FRANCHI I., SEXTON A. S., PILLINGER C. T. AND BISCHOFF A. (1998) Dar al Gani 400: Chemistry and petrology of the largest lunar meteorite (abstract). *Meteorit. Planet. Sci.* **33 (Suppl.)**, A171.